FAKULTA
STROJNÍ
ČVUT V PRAZE

Department of Automotive, Combustion Engine and Railway Engineering

Rear wing design and manufacturing for a Formula Student race car

BACHELOR'S THESIS
2024

Daniil Martynov

Study program:	B2342 TEORETICKÝ ZÁKLAD STROJNÍHO INŽENÝRSTVÍ
Study field:	2301R000 Studijní program je bezoborový
Thesis supervisor:	Ing. Petr Hatschbach, CSc., Ing. Martin Ševčík

BACHELOR'S THESIS ASSIGNMENT

I. Personal and study details

Student's name: **Martynov Daniil** Personal ID number: **493573**

Faculty / Institute: **Faculty of Mechanical Engineering**

Department / Institute: **Department of Automotive, Combustion Engine and Railway Engineering**

Study program: **Theoretical Fundamentals of Mechanical Engineering**

Branch of study: **No Special Fields of Study**

II. Bachelor's thesis details

Bachelor's thesis title in English:

Rear wing design and manufacturing for a Formula Student race car

Bachelor's thesis title in Czech:

Návrh a výroba zadního křídla pro závodní vůz Formula Student

Guidelines:

1. Competition Formula Student: history, rules, disciplines.
2. Reasons for designing a new generation of the wing for FS.14
3. Aerofoil design, overall wing shape choice and design, wing endplate design.
4. CFD flow calculation: description of calculation settings, evaluation of results.
5. Possibilities of experimental validation.

Bibliography / sources:

Name and workplace of bachelor's thesis supervisor:

Ing. Petr Hatschbach, CSc. Department of Automotive, Combustion Engine and Railway Engineering FME

Name and workplace of second bachelor's thesis supervisor or consultant:

Ing. Martin Ševčík ICON Technology & Process consulting s.r.o.

Date of bachelor's thesis assignment: **19.10.2023** Deadline for bachelor thesis submission: **10.01.2024**

Assignment valid until: _____

Ing. Petr Hatschbach, CSc.	doc. Ing. Oldřich Vítek, Ph.D.	doc. Ing. Miroslav Španiel, CSc.
Supervisor's signature	Head of department's signature	Dean's signature

III. Assignment receipt

The student acknowledges that the bachelor's thesis is an individual work. The student must produce his thesis without the assistance of others, with the exception of provided consultations. Within the bachelor's thesis, the author must state the names of consultants and include a list of references.

Date of assignment receipt _____ Student's signature _____

Summary

Name of the author:	Daniil Martynov
Name of the thesis:	Rear wing design and manufacturing for a Formula Student race car
Thesis volume:	32 pages
	39 figures
	4 tables
	9 plots
Academic year:	2023/2024
Department:	12 120 Department of Automotive, Combustion Engine and Railway Engineering
Study program:	Teoretický základ strojního inženýrství
Thesis supervisor:	Ing. Petr Hatschbach, CSc., Ing. Martin Ševčík
Key words:	Aerodynamics, Formula Student, wing

Abstract

This thesis is dedicated to designing and manufacturing a rear wing for FS.14, a race car of the CTU CarTech team. The main goals were increasing aerodynamic downforce of the vehicle and improving its stability. The thesis describes the flaws of the previous vehicle, the design approach, CFD simulations and the manufacturing methods, as well as the experimental validation of the final design.

Declaration

I, Daniil Martynov, hereby declare that I have written the thesis “Rear wing design and manufacturing for a Formula Student race car” independently with the use of professional literature and the sources specified in the list of used literature, the last chapter of the thesis.

Prague, 10.01.2024

……

(signature of the author)

Acknowledgement

I would like to thank my thesis supervisors, Ing. Petr Hatschbach, CSc. and Ing. Martin Ševčík, for the valuable advice and guidance in the process of writing this thesis, CTU CarTech aerodynamics group for the cooperation during the development, manufacturing and presentation of our designs, and Škoda Auto and 4Jtech for giving us an opportunity to experimentally validate our designs.

I would also like to thank my parents for giving me the opportunity to study in Czech Republic, and my brother, Ing. Nikita Martynov, for the lifelong guidance and support so necessary for the life abroad.

Contents

1 Introduction

1.1 CTU CarTech

CTU CarTech was the Formula Student team of the Faculty of Mechanical Engineering at CTU in Prague. The team designed and built 13 combustion-powered and 2 hybrid electric vehicles between 2007 and 2023. The thesis will be dedicated to the research and development done in the 2021-2022 season for the FS.14, the first generation of the hybrid electric vehicle. [1]

Figure 1: FS.14 [1]

1.2 Competition

Formula student is a race car design competition between universities all around the world held since 1981 [2]. The primary goal of the team is designing, manufacturing, testing, and racing a new vehicle each year. The disciplines of the competition are divided into 2 categories: static and dynamic. During the static events, the team presents the design concept of their vehicle, the financial documentation, and a fictional business plan. The static disciplines include Acceleration (75 m straight line), Skid pad, Autocross (a single lap on a racetrack), and Endurance (22 km on the racetrack with a driver change in the middle). During the Endurance, the fuel consumption (or electric energy consumption) is measured for ranking the teams in the Efficiency discipline. The maximum points that can be assigned are 675 for the dynamic disciplines and 325 for the static disciplines (see figure 2). As the dynamic disciplines are evaluated by the lap time, it is crucial to invest in development that can improve dynamic performance. [3]

Static Events:	
Business Plan Presentation	75 points
Cost and Manufacturing	100 points
Engineering Design	150 points
Dynamic Events:	
Skid Pad	50 points
DV Skid Pad	75 points
Acceleration	50 points
DV Acceleration	75 points
Autocross	100 points
DV Autocross	-
Endurance	250 points
Efficiency	75 points
Trackdrive	-
Overall	1000 points

Figure 2: Points assigned for each discipline [3]

1.3 Rules

The most important condition for scoring points in the dynamic disciplines is the vehicle's compliance with the competition rules in terms of the technical regulations at any moment of the competition, including inspections after the runs. In this thesis, I would like to pay attention to the rules regarding the aerodynamic devices.

An aerodynamic device is defined as component of the vehicle made with the purpose of producing aerodynamic downforce or/and reducing the aerodynamic drag, such as wings, sidepods, Venturi tunnels and diffusers. According to the 2022 Formula Student Germany rule set, the aerodynamic devices are restricted by 3 general rules: minimum edge radii for the edges that might contact a pedestrian (3 mm for vertical edges and 5 mm for horizontal edges), sufficient strength and rigidity to withstand pressure or point force with a specified maximum deflection, and the size and shape constrained by the envelopes. The envelope of the rear wing is 1200 mm tall and is restricted by inner tyre surfaces on the sides, driver's headrest in the front and a plane 250 mm behind the rear tyre in the back (see figure 3). [3]

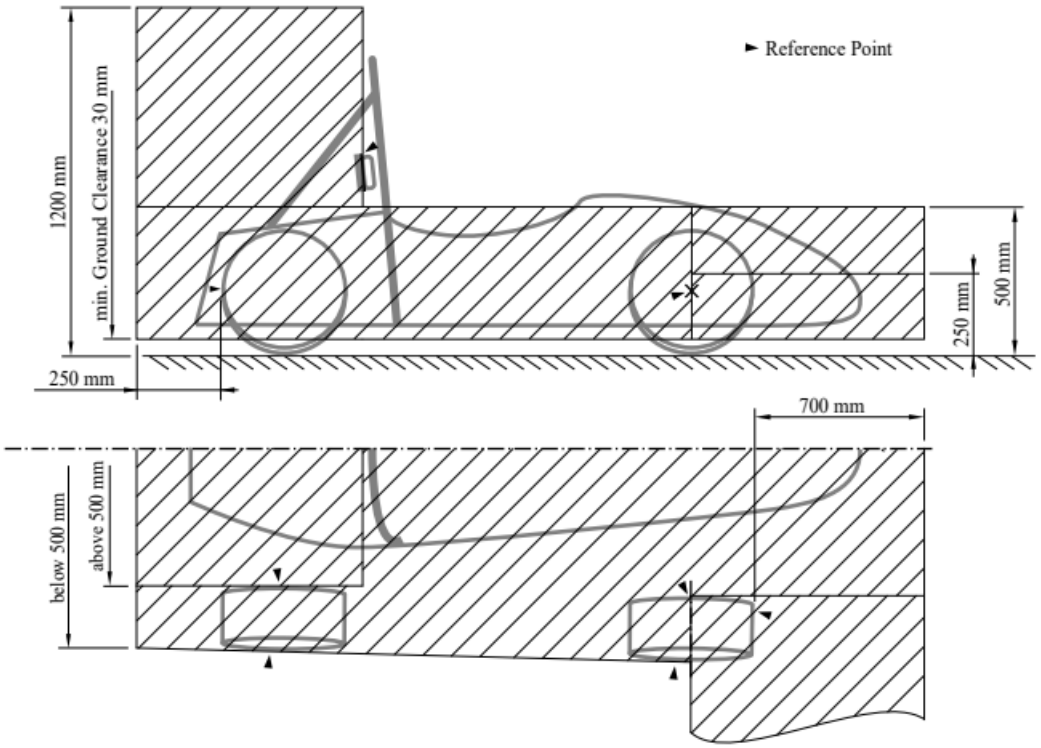

Figure 3: Envelopes of the aerodynamic devices [3]

2 Theoretical base

2.1 Aerodynamic forces

Aerodynamic forces are the forces acting on the vehicle due to the upcoming air. The forces are created by pressure (forces normal to the surface) and friction or sheer stress (forces tangent to the surface). The overall force is split into 3 components: lift force on the vertical axis, drag force opposite to the direction of movement and a side force perpendicular to the direction of movement (see figure 4).

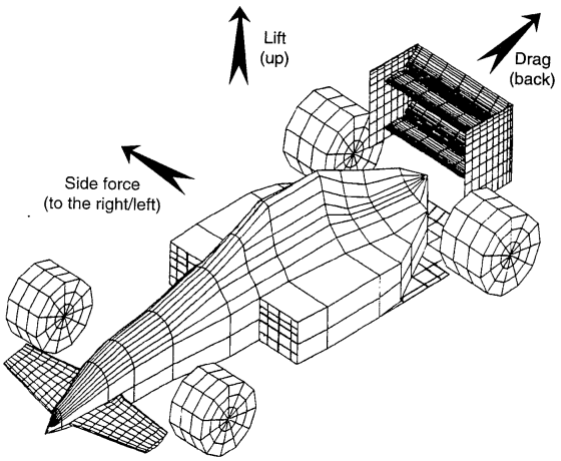

Figure 4: Aerodynamic forces and their directions [5]

The aerodynamic lift can be presented by the following equation:

$$F_l = \frac{1}{2} C_l * A * \rho * v^2 \ [N] \tag{2.1.1}$$

Where C_l is the dimensionless coefficient of lift defined by the vehicle shape, A is the vehicle's frontal area, ρ is the medium density and v is the velocity of the medium relatively to the vehicle.

The aerodynamic drag is defined by a similar equation:

$$F_d = \frac{1}{2} C_d * A * \rho * v^2 \ [N] \tag{2.1.2}$$

Where C_d is the dimensionless coefficient of drag.

In order to evaluate the air pressure independently from the vehicles velocity, dimensionless pressure coefficients are used:

$$C_p = \frac{p - p_\infty}{\left(\frac{1}{2}\right) * \rho * {v_\infty}^2} \ [-] \tag{2.1.3}$$

Where p is the pressure at the given point, p_∞ is the atmospheric and v_∞ is the free stream velocity.

Another important coefficient is the total pressure coefficient. The total pressure is the sum of the static pressure and the dynamic pressure:

$$p_{Total} = p + \left(\frac{1}{2}\right) * \rho * {v_\infty}^2 \ [Pa] \tag{2.1.4}$$

$$C_{p_{Total}} = \frac{p_{Total} - p_\infty}{\left(\frac{1}{2}\right) * \rho * {v_\infty}^2} \ [-] \tag{2.1.5}$$

A decrease in the total pressure is a marker of the air losing energy due to friction or flow separation. [5]

2.2 The importance of the aerodynamic downforce

The aerodynamic downforce (or negative lift force) allows race cars to exert higher acceleration in all directions by increasing the normal force on the tires, hence the maximum friction force. [5] This is especially important in Formula Student, as the racetracks require frequent cornering, braking and acceleration. An experiment held by CTU Cartech on the FS.11 (race car from the 2019 season) defined that removing front and rear wings from the vehicle with the side tunnels still attached resulted in increasing its lap time on a **594 m** test track by **0.977** seconds. [6]

Figure 5: FS.11 [6]

Figure 6: FS.11 without front and rear wings [6]

2.3 Centre of pressure position

The centre of pressure is a theoretical point where the overall aerodynamic force is applied to the vehicle. For achieving aerodynamic stability, the centre of pressure must be located behind the centre of gravity (see figure 7). One of

the ways to ensure this is to compare the aerodynamic load percentage on the front axle to the gravitational load percentage.

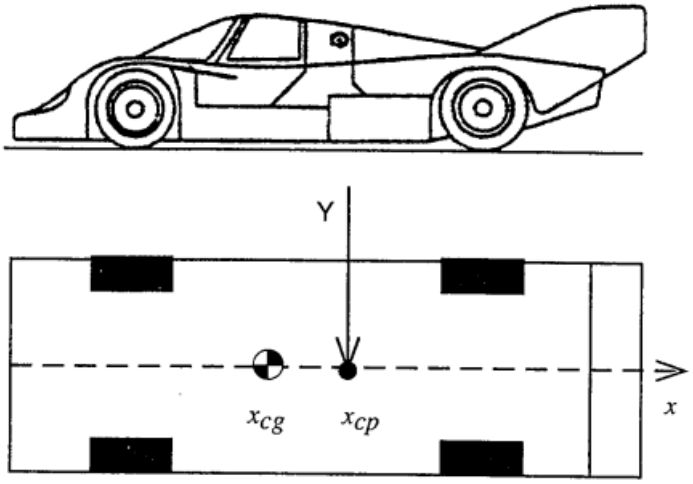

Figure 7: A typical centre of pressure position (x_{cp}) and centre of gravity position (x_{cg}) on a race car [5]

2.4 Aerofoil theory

An aerofoil is a two-dimensional cross section of a three-dimensional wing. The foremost point of an aerofoil is referred to as the leading edge, and the rearmost as trailing edge. The line connecting these points is called the aerofoil's chord (*c* in figure 9). The width of a three-dimensional aerofoil is referred to as span (*b* in figure 8). Aerofoils can be symmetric relative to the chord or cambered.

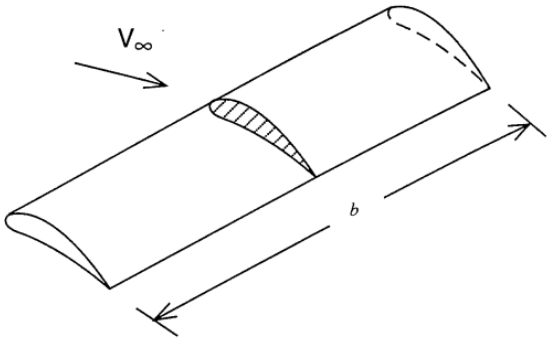

Figure 8: Cross-section of a 3-dimenisonal wing [5]

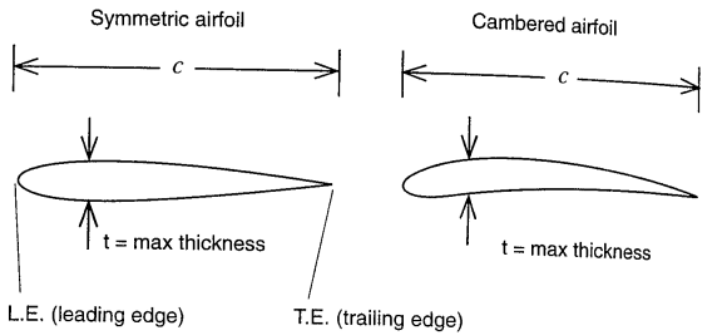

Figure 9: Basic aerofoil nomenclature [5]

The angle between the free stream velocity vector and the aerofoil chord is called the angle of attack.

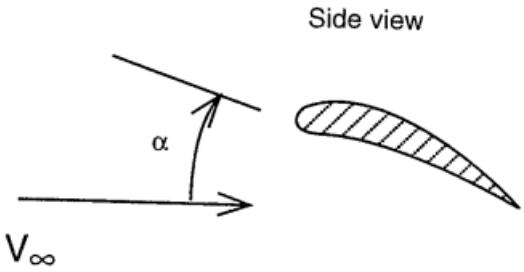

Figure 10: Angle of attack [5]

Another important point on an aerofoil is the stagnation point: in this point, the upcoming air does not flow under or over the aerofoil, but stops or stagnates.

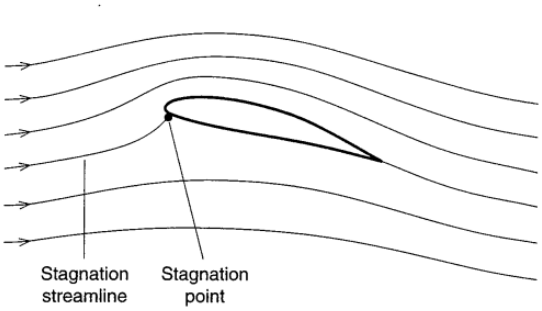

Figure 11: Stagnation point [5]

The pressure distribution on the aerofoil is the main parameter defining its performance. The tool used most often is a plot showing the pressures (or pressure coefficients) on the upper and lower surfaces of the aerofoils on the vertical axis and the aerofoil chord or X-coordinate on the horizontal (see figure 12). The vertical force is then defined by the area inside the plot.

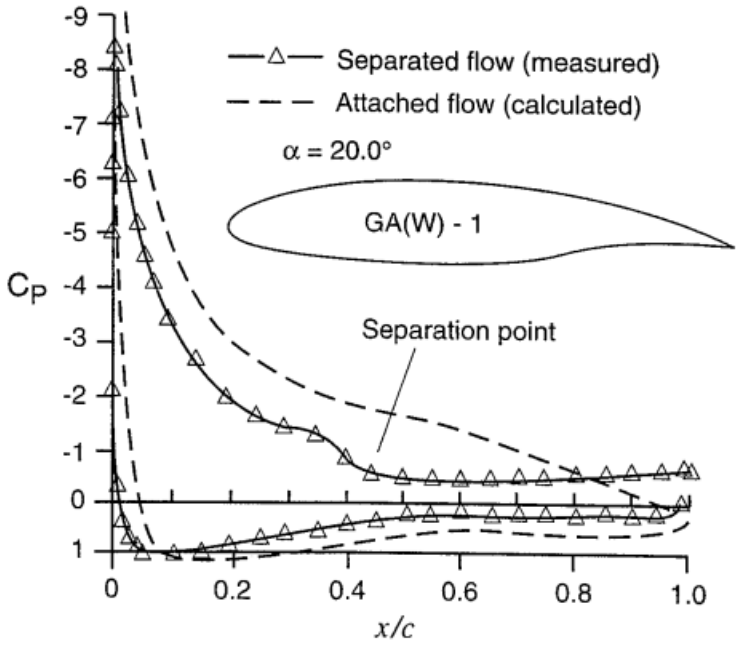

Figure 12: An example of a pressure distribution plot for a GA(W) - 1 aerofoil [5]

The main limitation in aerofoil design is stalling or flow separation. It is caused by recirculation of the airflow in the boundary layer. The recirculation is caused by the adverse pressure gradient: an increase in pressure in the direction of the airflow. To avoid stalling, the pressure must grow gradually to create a favourable pressure distribution.

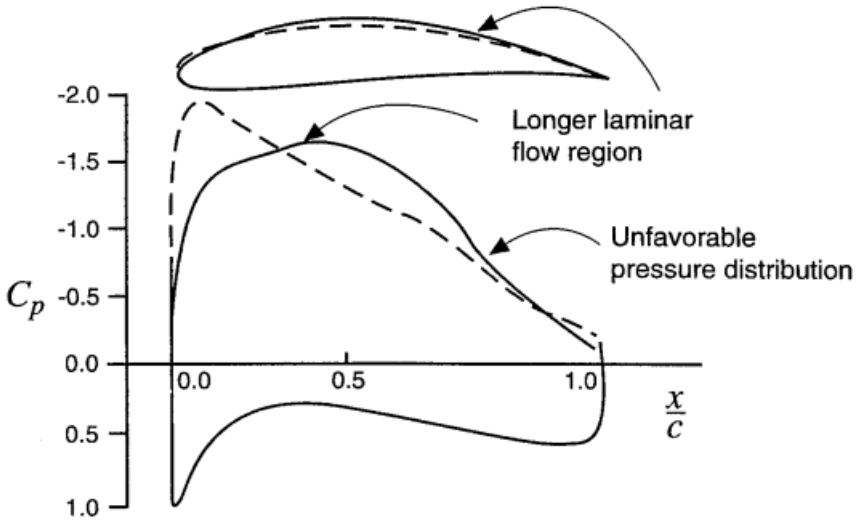

Figure 13: Favourable (dotted line) and unfavourable (full line) pressure distribution on an aerofoil [5]

The pressure is most often dependent on curvature: convex curvature causes a decrease in pressure; concave causes an increase. To achieve the optimal pressure distribution, the curvature of the suction surface must decrease gradually along the aerofoil chord. [5]

2.5 Multi-element wings

In order to achieve maximum lift force without flow separation, multiple aerofoils are used in a series. This allows to prevent the boundary layer growth as opposed to a single-element wing. [5]

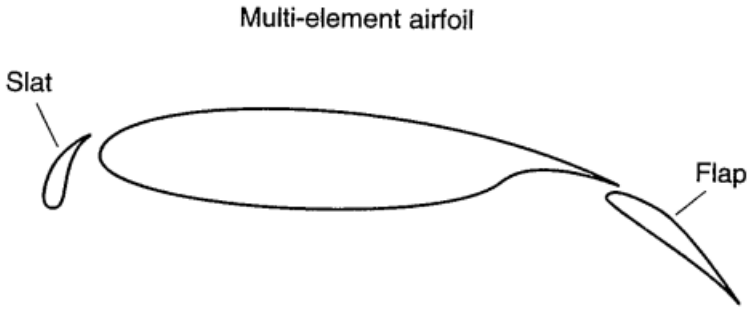

Figure 14: Multi-element aerofoil [5]

2.6 Finite wings

The 2-dimensional approach to the aerofoil design is not precise due to the finite nature of the wing. The pressure difference between the suction and pressure sides of the aerofoils causes the air to flow around the wingtips, thus producing strong vortexes. This behaviour leads to a decrease in the lift force and a high increase in drag force. In order to decrease the influence of the wingtip effect, end plates are used.

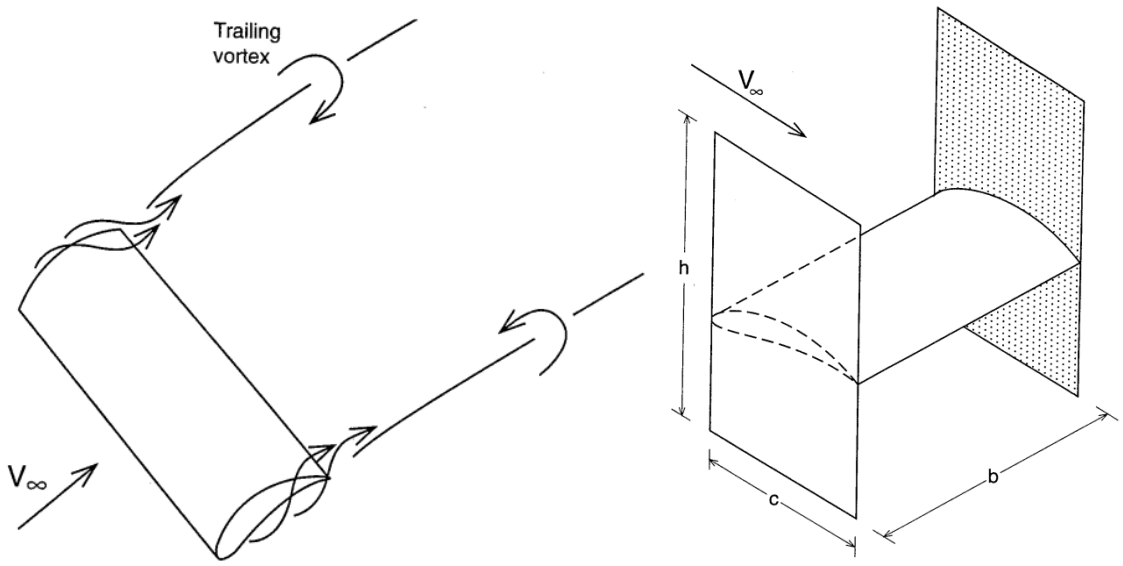

Figure 15: Trailing vortices formed on the wing tips (left) and simple end plates (right) [5]

3 CFD model reference

3.1 2D model

The 2D model used for early simulation was created in Siemens STAR CCM+ and has the following properties:

- 30 m/s air velocity (approximate maximum speed during Autocross and Endurance) at 5° angle upwards
- SST K-omega turbulence model
- Steady-state RANS equations
- Polyhedral mesh
- 15 prism layers
- Volume refinement with 2 bodies of influence

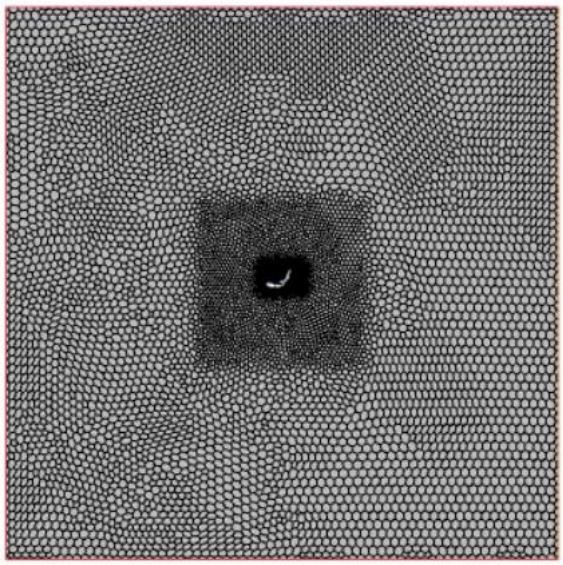

Figure 16: 2D CFD full domain mesh

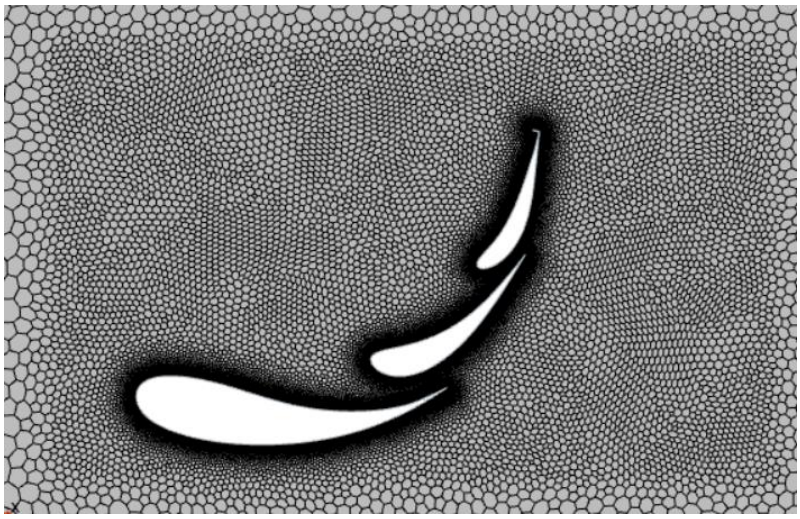

Figure 17: 2D CFD mesh in detail

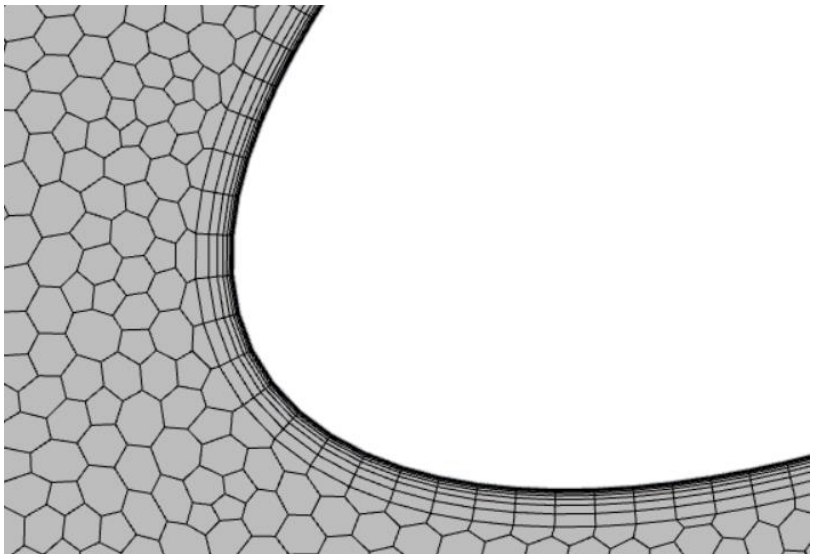

Figure 18: Prismatic layers in the 2D CFD mesh

3.2 3D model

The 3D CFD model used in CTU CarTech is a simulation in Siemens STAR CCM+ software with the following parameters:

- Left half of the car
- 15 m/s air velocity (average speed during Autocross and Endurance)
- Realizable K-ε turbulence model
- Steady-state RANS equations
- Boundary layer modelled with wall functions
- Trimmer and polyhedral mesh
- 2 prism layers
- Volume refinement with 4 bodies of influence

- Blockage ratio under 1%
- Rotating wheels, moving road
- Multiple Reference Frame function used in wheel rims, brake discs and cooling fans

The aerodynamic package performance is evaluated through coefficients of lift (Cl) and drag (Cd) of the complete vehicle and separate assemblies with the reference area of 1.031 m^2. The other parameters include the percentage of the aerodynamic load on the front axle and cooling mass flow. [6]

Note: as the model was used for simultaneous development of the complete aerodynamic package, the direct comparison between different rear wing versions is not always possible. You will find a detailed description of the gains made by the end of development in the section 4.7.

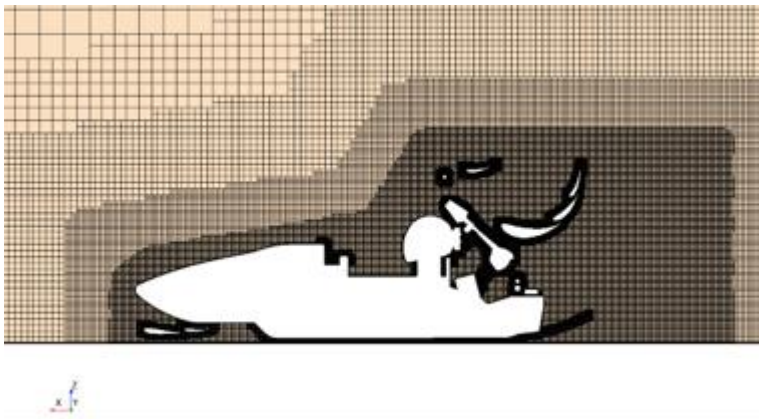

Figure 19: Volume mesh around the car

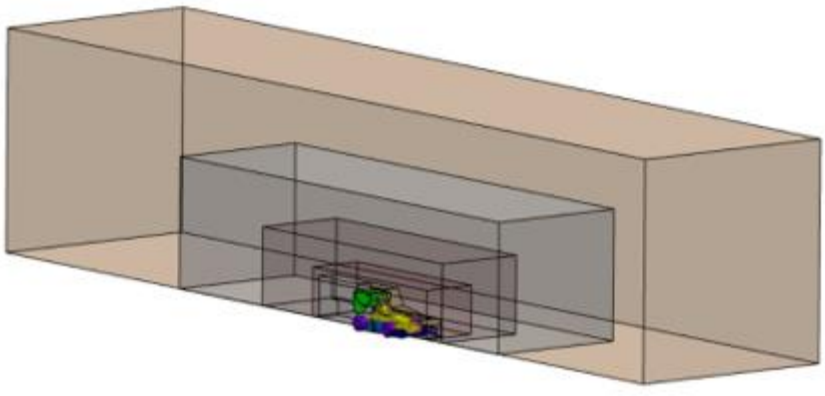

Figure 20: Bodies of influence used for volume refinement

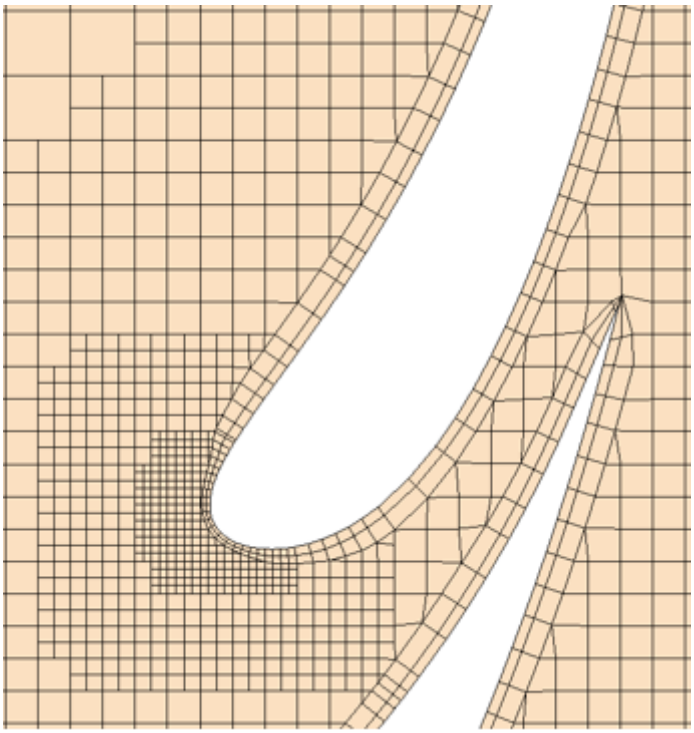

Figure 21: 2 Prismatic layers on the rear wing elements

4 Design objectives

The FS.13 was the vehicle built for the 2021 season. For creating its successor, the aerodynamics group of CTU CarTech pinpointed the main design flaws of the aerodynamic package:

- Low aerodynamic downforce: the FS.13 had the Cl*A of only **2,9**, while the most recognised teams, such as Rennstall Esslingen and Rennteam Stuttgart claimed Cl*A of **5,2** on their race car from the same season, while having similar vehicle dimesions. [4]
- Aerodynamic balance shifted to the front of the car: while the weight distribution of the FS.13 was **49%** to the front axle, the aerodynamic downforce at the front was as high as **59,6%** Such distribution resulted in oversteering at higher speeds, according to the drivers' feedback.
- Usage of aircraft aerofoils available in an open-source database. Such aerofoils are focused on a high aerodynamic efficiency instead of high lift and might not be optimal for the motorsport application and encouraged us to try custom aerofoil shapes made with the help of curvature analysis in CAD software.

Taking all the above into consideration, we made the decision to design a completely new aerodynamic package for the FS.14, my task being the development of a rear wing based on custom aerofoils.

5 Design

5.1 Aircraft aerofoil problematic

The aerofoils used in aviation all have a very high efficiency factor:

$$AE = \frac{C_l}{C_d}\ [-]\ [5] \tag{5.1.1}$$

The efficiency factor is crucial for aircraft aerofoils as it defines the flight time and load capacity.

The aerofoil historically used in CTU CarTech on every rear wing element is a Selig aerofoil, S1223 (see figure 22). Among aircraft aerofoils, Selig are considered to provide the most lift (higher Cl) at the cost of lower aerodynamic efficiency. Even the S1223, however, can reach the efficiency of over 100 at most of the operational angles of attack (see plot 1). This fact made me assume that custom aerofoils with higher lift can be created at the cost of a lower aerodynamic efficiency. [7]

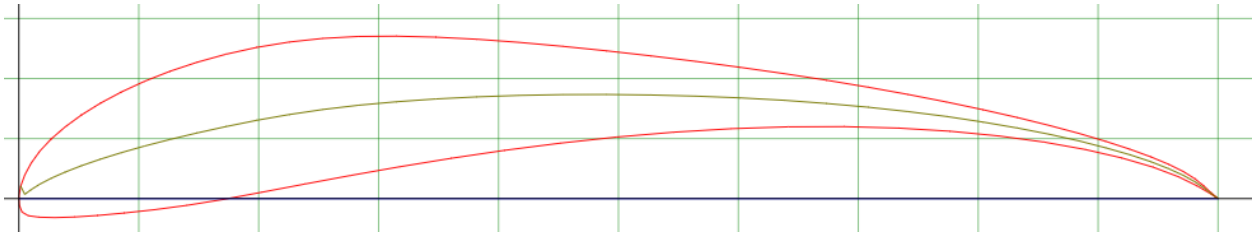

Figure 22: S1223 aerofoil [7]

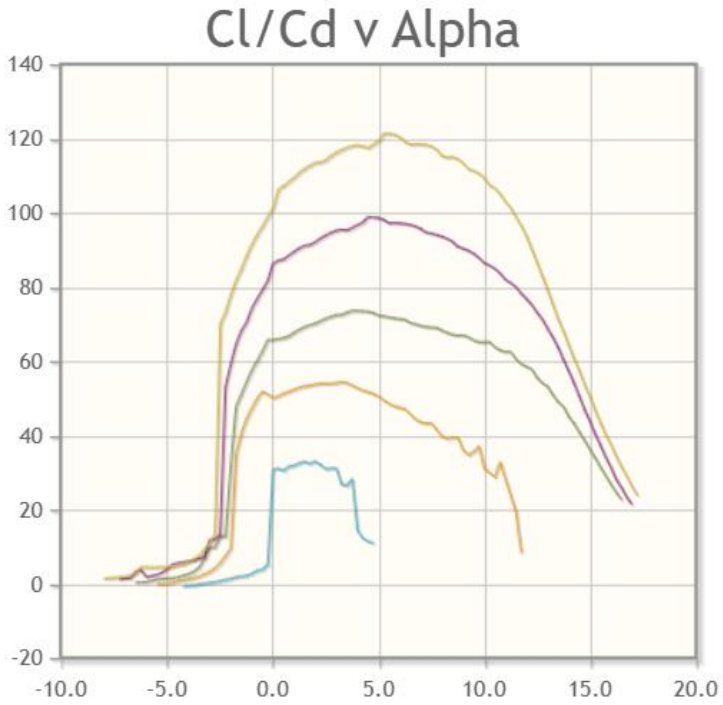

Plot 1: S1223 aerodynamic efficiency at various angles of attack [7]

Moreover, most of the aircraft aerofoils are optimized for single-element wings, whilst in motorsport, most of the wings consist of multiple elements permanently arranged in a series.

5.2 Design approach

The tool used for design is a curve defined by control points and porcupine curvature analysis. This tool allowed us to shape the aerofoils with desired curvature in every point. With the help of the 2D CFD simulations, each concept could be tested multiple times in a trial-and-error approach. The individual points could be moved to achieve the desired local shape.

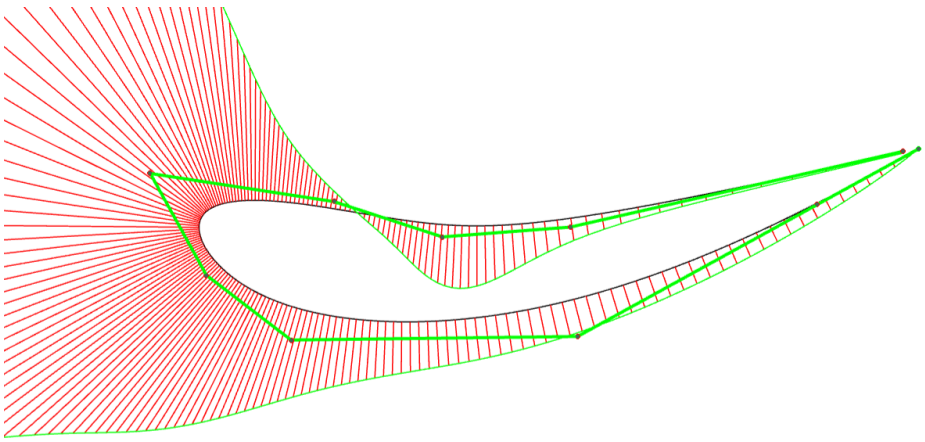

Figure 23: An example of a custom aerofoil: the curvature is represented by the length of the red lines, the control points are the vertices of the green polygon

5.3 Envelope definition

The available envelope for the wing is a pentagon: most of sides are defined by the rules, and one by the engine air intake. This shape presents a problem in design approach: the wing can either be longer in X-axis or taller in Z-axis. To address this problem, 3 shapes of the envelope were used, limited by a lower surface: 50 mm above the previous design, similar height, and 50 mm below, or 620, 570 and 520 mm in Z axis respectively. I used a two-dimensional CFD simulation to create 3 series of aerofoils. For each variant, I have created 10 to 20 versions, trying to achieve maximum performance, while keeping a favourable pressure distribution on the wing.

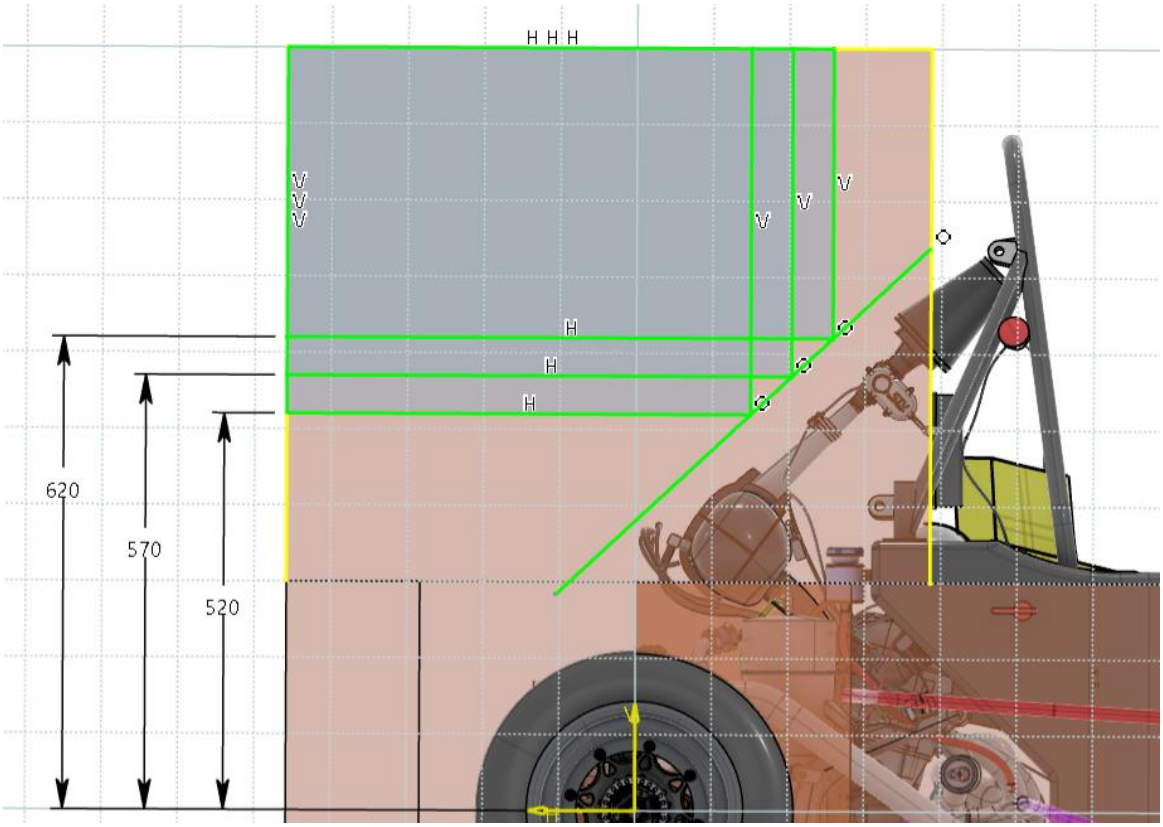

Figure 24: Rear wing envelopes

5.4 Envelope comparison

The aerofoil geometry used for envelope comparison can be seen in the pictures below.

Figure 25: Aerofoil geometry for various envelopes: 520 mm – 570 mm – 620 mm

The results are lift and drag forces in newtons at the velocity of 30 m/s are presented in the table 1. As you can see, the performance is quite similar in the 2D model. The pressure plots show a favourable pressure distribution along the wing.

Lower plane Z coordinate [mm]	Lift [N]	Drag [N]
520	-1308	187
570	-1335	166
620	-1388	156

Table 1: Rear wing performance comparison in a 2D simulation

The next step was comparing these concepts in a 3D CFD simulation including the full car model to realistically evaluate the wing performance. The resulting coefficients of drag and lift are presented in the table 2.

	Lower plane Z coordinate [mm]	520	570	620
Whole vehicle	Cd [-]	1,253	1,173	1,099
	Cl [-]	-3,919	-3,803	-3,669
Rear wing	Cd [-]	0,535	0,473	0,465
	Cl [-]	-1,273	-1,216	-1,268

Table 2: Rear wing performance comparison in a 3D simulation

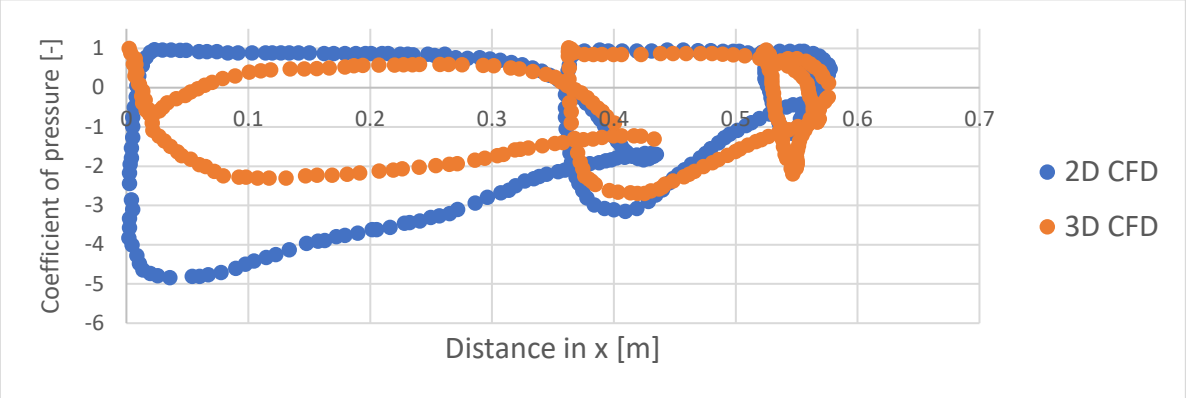

Plot 2: Pressure distribution on the 520 mm version

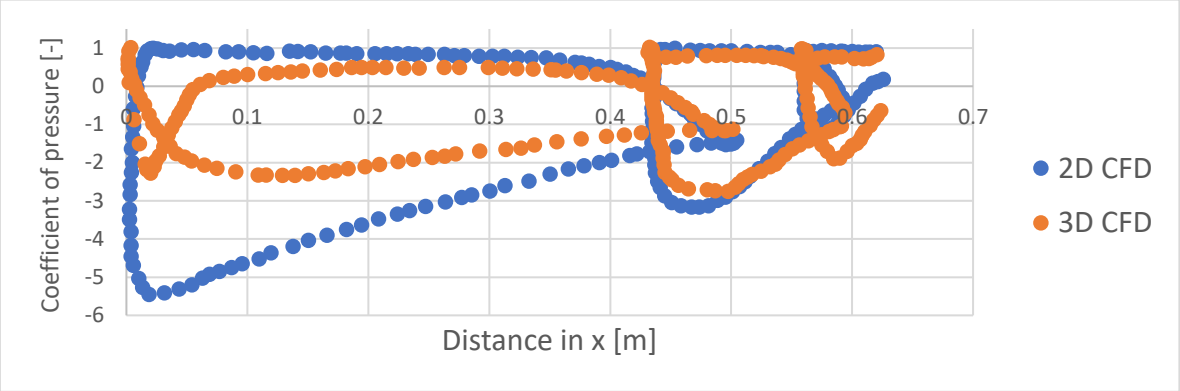

Plot 3: Pressure distribution on the 570 mm version

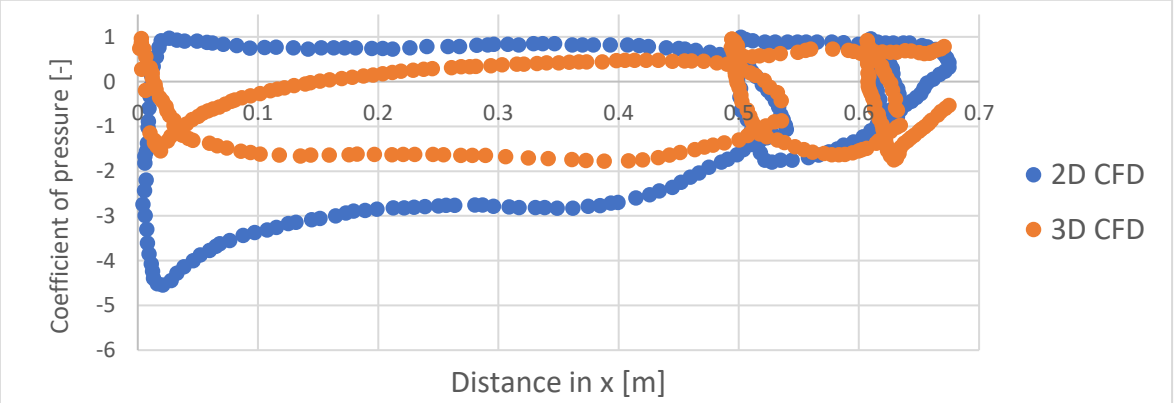

Plot 4: Pressure distribution on the 620 mm version

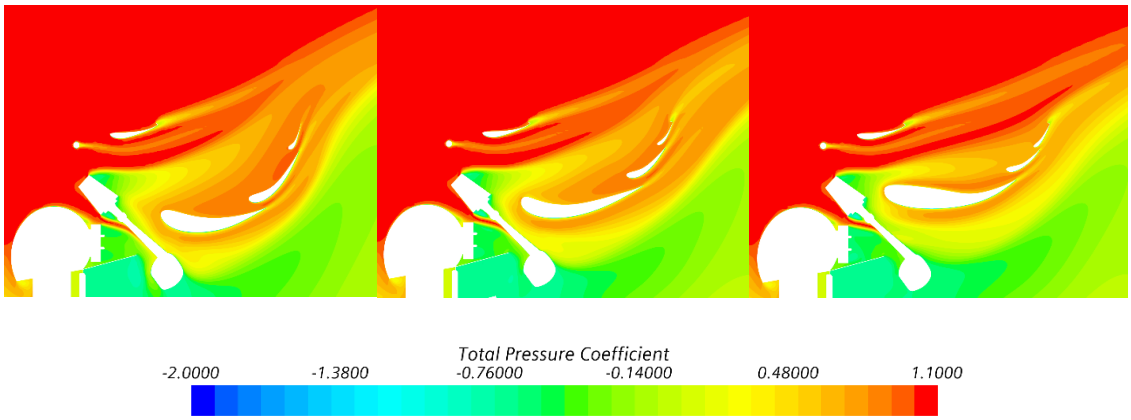

Figure 26: Total pressure coefficient in XY plane section on the 3 wing variants (520 mm – 570 mm – 620 mm)

As you can see, the 520 mm concept ensures the best lift coefficient on the whole car. The behaviour of the wing is very different from the 2D simulations (see plots 2 – 4). The first element has a much lower suction on the bottom side compared to the 2D simulations. The angle of attack doesn't appear correct. The third and second elements' behaviour correlates to the 2D model more accurately. The difference in results can be caused by several factors:

- Interaction with the top surface of the chassis, sidepods, driver's helmet, and air intake: these parts are omitted in the 2D model and can cause a change in the angle of attack and the total pressure of the airflow (see figure 26)
- The effect of the finite width of the wing (2D model simulates an infinitely wide wing).
- Interaction with the wing end plates.
- Interaction with the upper front element – left from FS.13 in early variants.

Further development was based on the 520 mm baseline and included 2D simulations for studying the interaction between the elements and 3D simulations for adapting the wing to the realistic conditions.

5.5 Final shape

Judging by the pressure distribution plots, the most problematic element is the first one. Its performance is strongly dependent on the shape of the driver's helmet, chassis and engine air intake. The angle of the upcoming air is not only different from the 2D simulations, but also varies along the wing. The next task was optimizing the wing in order to perform correctly in these complex conditions.

As the airflow doesn't meet the wing at the constant angle, a non-constant shape of the aerofoils is often used in motorsport. In order to create such an element, 2 different aerofoils were used: one in the middle section and one near the endplate, connected by a transient shape. In the table 3 you can find the comparison of an optimized straight first element and a curved first element.

	Straight	Curved
Cl*A: overall [m^2]	-3,716	-3,738
Cd*A: overall [m^2]	1,532	1,547
Cl*A: rear wing [m^2]	-1,042	-1,084
Cd*A: rear wing [m^2]	0,596	0,604

Table 3: Straight and curved first element comparison

In the plots and figures below you can see the comparison of performance of the FS.13 and FS.14 wings. The overall coefficient comparison can be found in 5.7.

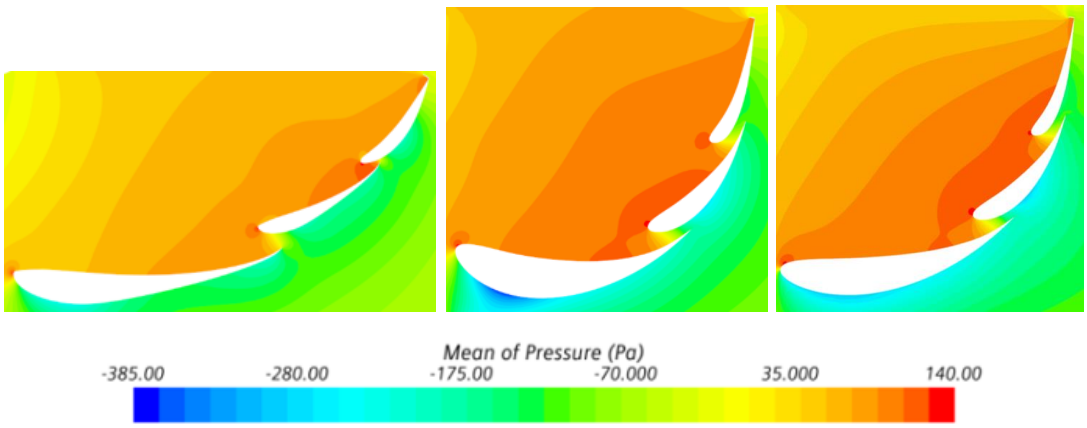

Figure 27: Pressure near of the wing (FS.13 on the left, FS.14 middle section in the middle, FS.14 side section on the right)

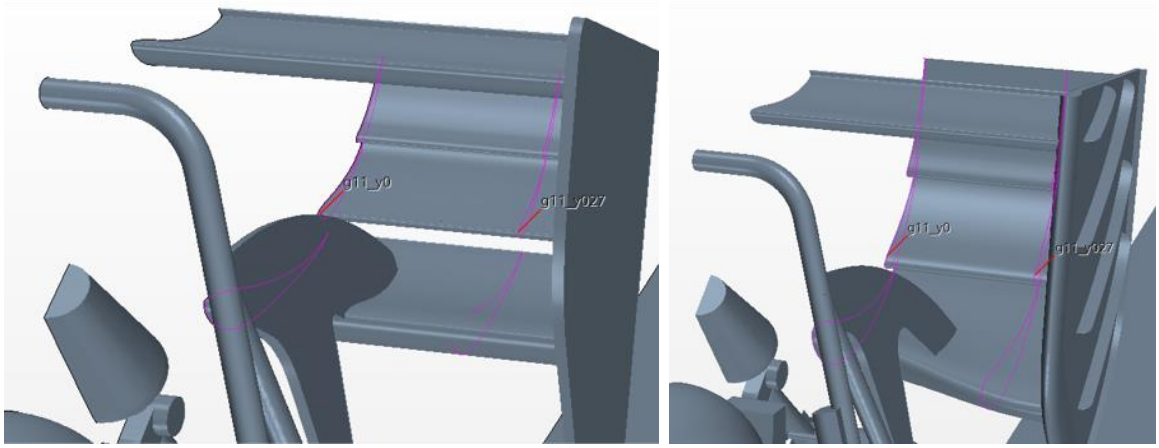

Figure 28: Rear wing geometry (FS.13 on the left, FS.14 on the right); purple line to mark the section positions

The pressure plots 5 and 6 on the FS.14 aerofoils shows a much larger area inside the lines that should lead to a higher aerodynamic downforce (see 5.7 for

the overall numerical results). Moreover, the pressure grows gradually along the wing, creating a favourable distribution and theoretically ensuring attached flow.

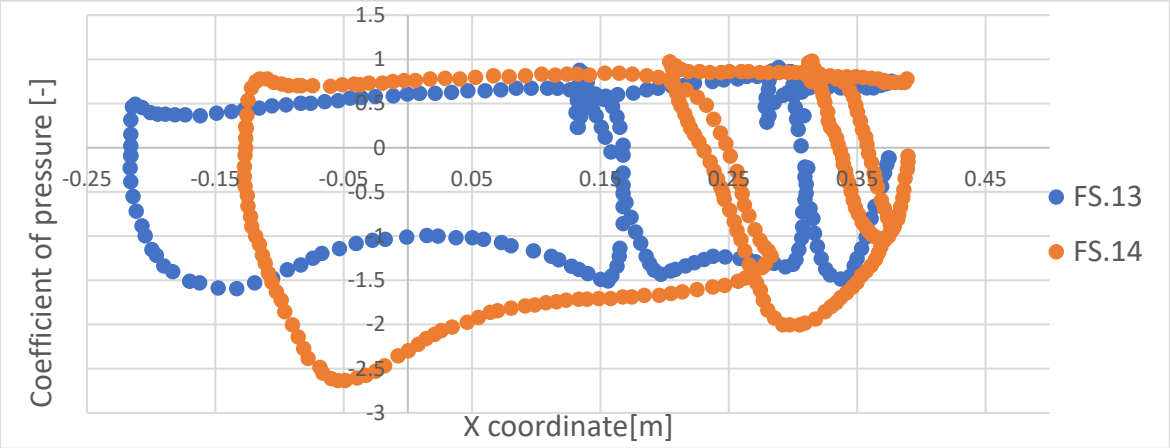

Plot 5: Pressure distribution in the middle section of the wing

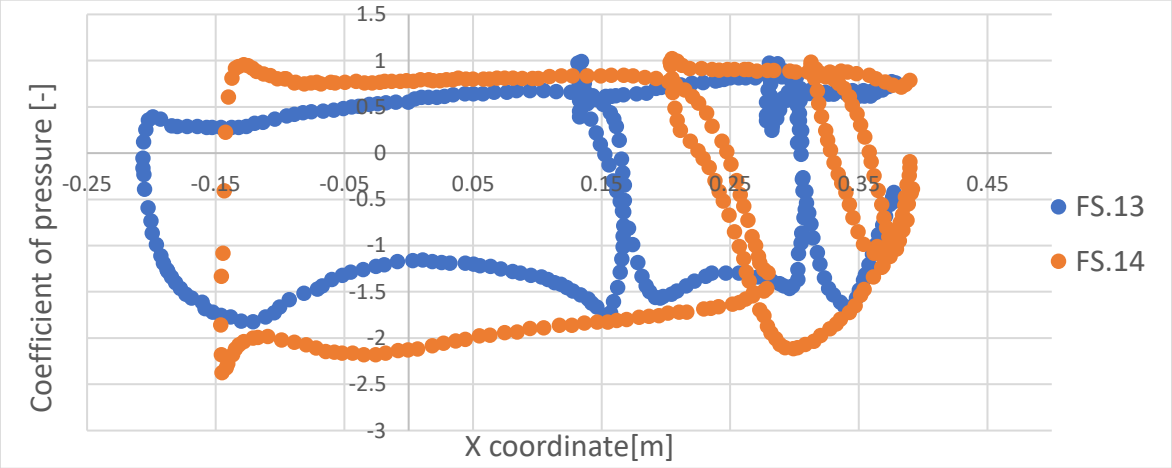

Plot 6: Pressure distribution 270 mm away from the centre

5.6 End plate design

Wing end plates are the vertical surfaces used to keep the pressure above and below the wing isolated from each other and the air outside the wing. The previous end plate design was a simple flat panel (see figure 29). The blunt edges of the end plate caused flow separation on the inside. The first changes made to the end plate included:

- An aerofoil-like nose to prevent separation.
- A flat perpendicular plate behind the endplate to increase the suction under the wing (see figure 30).

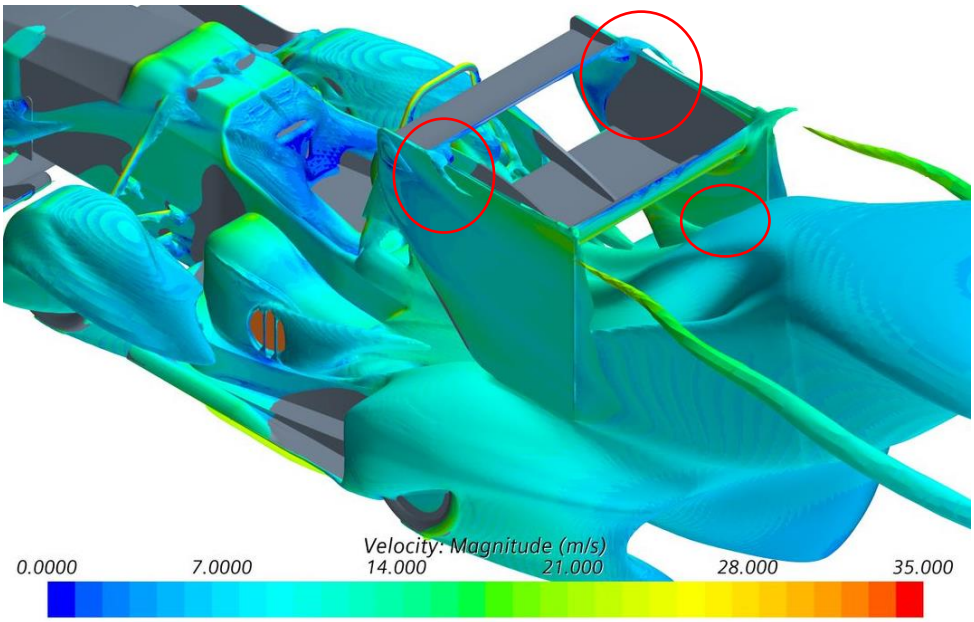

Figure 29: An isosurface of the zero total pressure - previous end plate design

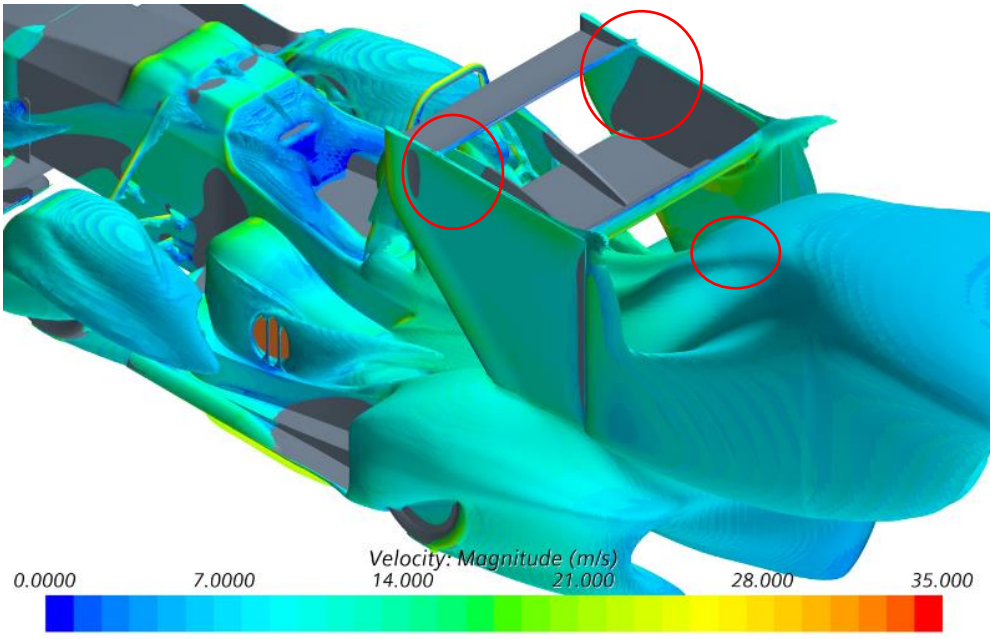

Figure 30: An isosurface of the zero total pressure: new end plate version

Such change on the end plates resulted in lower amount of flow separation under the wing and a 1,5% increase of the downforce for the complete vehicle compared do the old end plate version. In the pictures above you can see the isosurface of the zero total pressure – a strong marker of the flow separation. Note the changes in the circled areas.

The other concept implemented on the end plates was a series of vortex generators. With the new end plate nose shape and a flat plate protruding to the outside, a space on the outer side of the end plate was now available. The vortex generators benefits from the low pressure on their lower side and lead to a 1,5%

downforce increase on the complete vehicle compared to a similar end plate without the vortex generators (see figures 31 – 32).

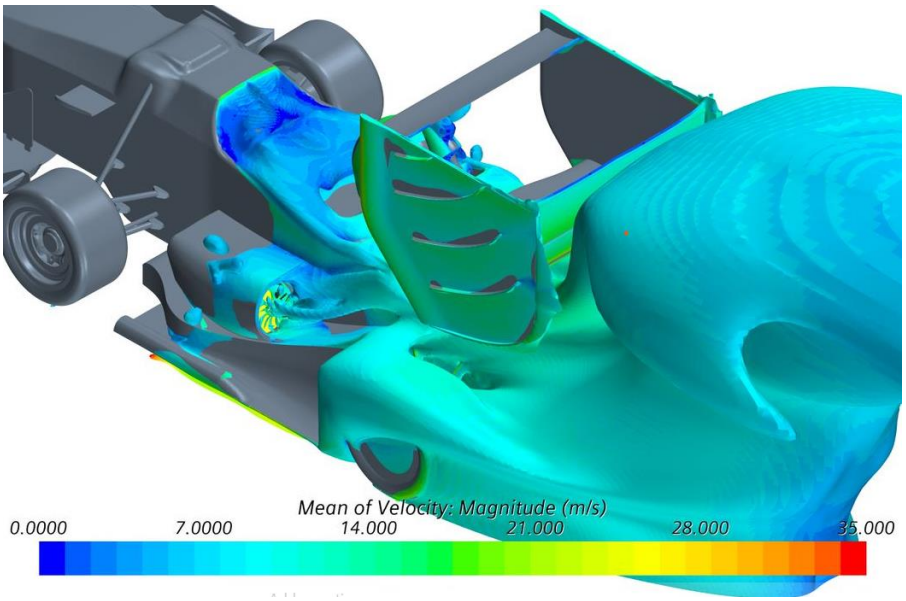

Figure 31: An isosurface of the zero total pressure: end plates with the vortex generators

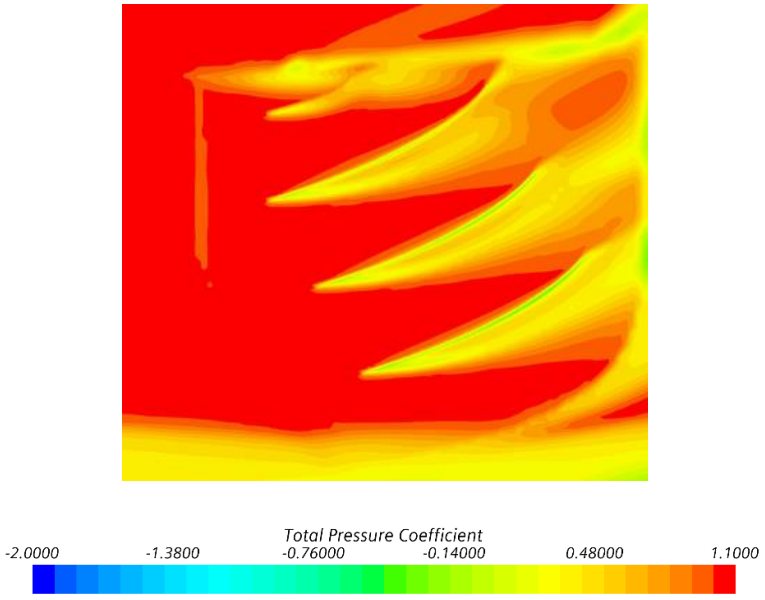

Figure 32: Total pressure coefficient near the end plate and the visible vortices

5.7 Overall aerodynamic package results

According to the CFD simulations, the development done on the aerodynamic package for the FS.14 resulted in the following gains:

	FS.13	**FS.14**
Cl*A [m^2]	-2,891	-4,052
Cd*A [m^2]	1,228	1,605
Cl*A/Cd*A [m^2]	2,354	2,524
Cl*A front wing [m^2]	-1,296	-1,136
Cl*A side tunnel [m^2]	-0,390	-1,140
Cl*A rear wing [m^2]	-1,103	-1,367
Front axle load [%]	59,6	46,4

Table 4: FS.13 and FS.14 aerodynamic performance

As you can see, the overall Cl*A increased by 40%. The load distribution shifted from 59,6% to only 46,4% on the front axle. Thus, the goals set for the aerodynamic package design can be considered achieved.

6 Manufacturing

6.1 Moulds

Milled MDF moulds were used for the majority of the parts of the aerodynamic package. The moulds were impregnated with epoxy resin and painted with an automotive grade paint. The painted surfaces were then sanded and polished. For parts with complex shape, the moulds were assembled from several parts. For example, you can see the mould of the first element of the rear wing in the figure 33: the side moulds are 3D-printed using PLA filament. The side moulds also define the position of the threaded inserts. Some of the moulds (such as the end plate and holder moulds) were cut out of sheet aluminium.

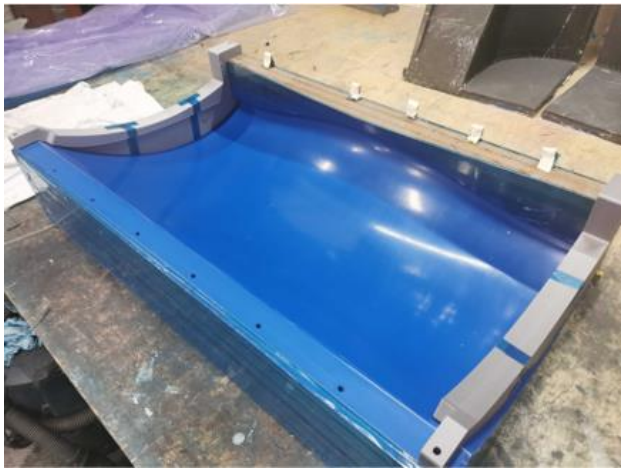

Figure 33: First element mould

6.2 Lamination

Most of the parts of the rear wing were laminated using the wet layup method, a relatively cheap and simple lamination technology [8]. The dry carbon fibre was applied to the moulds layer by layer with epoxy mixed with hardener added to each layer. The used layups were 1 layer of 180 g/m^2 spread tow carbon fibre and 1 layer of 200 g/m^2 twill carbon fibre for all surfaces except the wing sides: they had 4 layers of 200 g/m^2 twill carbon fibre to withstand the load near the inserts . The parts were then covered with peel-ply, perforated foil and breather fabric and sealed in a vacuum bag. The parts were cured overnight at room temperature.

The wing holders, being a structurally important part, were laminated out of prepreg carbon fibre: fibres industrially impregnated with epoxy. Such material possesses lower weight and higher strength, but its price allows us to use it only for the critical parts [8]. The holders were laminated in one piece, with 2 layers of 200 g/m^2 twill carbon fibre, a Rohacell IGF-31 foam core and nylon inserts around the fastener holes (see figure 34). The holders were put between two identical sheet aluminium moulds and sealed in a vacuum bag. They were then cured in an oven at 130˚C.

Figure 34: Rear wing holder lamination

6.3 Assembly

The laminated parts were glued together inside the moulds. The majority of the wings had packaging polystyrene as core. Such material is one of the lightest available for this application at the density of 15 to 20 kg/m^3. Unfortunately, we were not able to find a way to mill the polystyrene, so the only available technology was wire-cutting. The wire-cut cores were usable for the smaller

wing elements, however the first element, given its complex shape, had 9 Rohacell foam ribs instead of a full core (see figure 36).

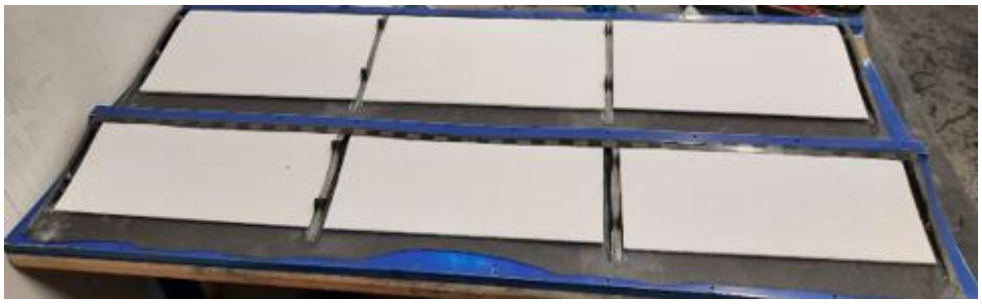

Figure 35: Polystyrene core inside the front wing

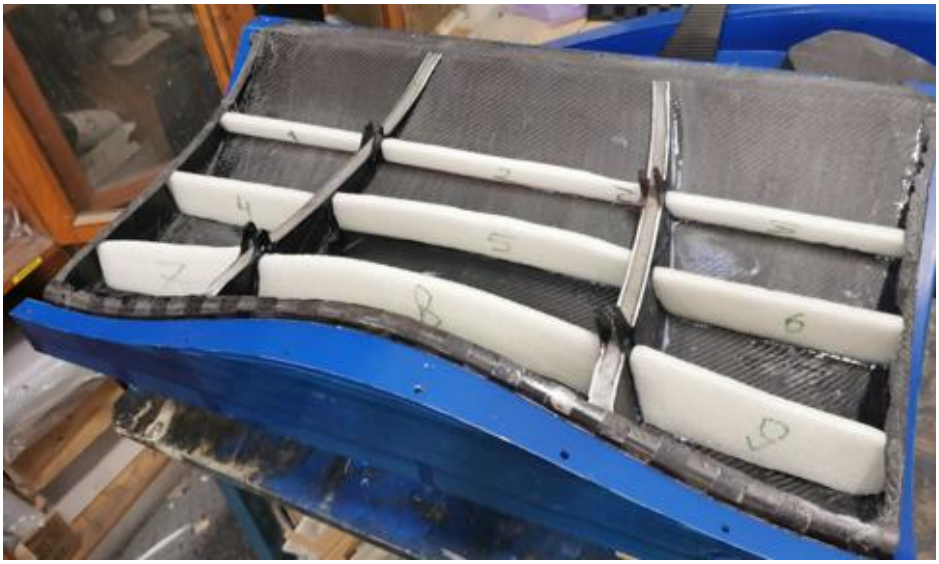

Figure 36: Inner structure of the first element of the rear wing

In order to provide higher adhesion quality between the carbon fibre composite and the polysterene core, a foaming epoxy resin was used instead of glue on the majority of the surfaces. In the places where carbon fibre adhered directly to carbon fibre, epoxy glue was used. With the parts locked tightly inside the moulds, the foaming epoxy filled the crevices inside the part and provided a hard layer between the core and the carbon fibre. [8]

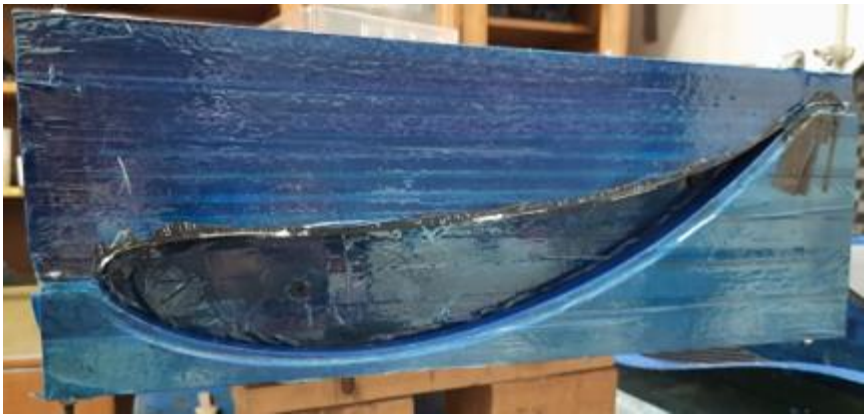

Figure 37: Wing locked in the mould for gluing

Every wing element had 2 riveted nuts on each side and the wing was assembled using countersink bolts.

7 Validation

7.1 Pressure strip test

The measurements described in this chapter were performed by my colleagues from the aerodynamics group and specialists from Škoda Auto and 4Jtech at a Škoda testing facility. The main means of validation for us was the pressure strip test. Absolute pressure sensors arranged on a plastic ribbon are applied to various vehicle surfaces and the pressure distribution is measured. The vehicle drives back and forth on a runway with constant velocities, and the mean pressures are recorded. The pressures can later be plotted and compared to the CFD simulation results. The CFD simulation has to be run at the conditions similar to the experiment: ride height of the vehicle, air velocity and atmospheric pressure. Air velocity can be measured with a pitot tube placed on the nose of the vehicle, but strong side wind should be avoided. You can see the sensors arranged on the rear wing in the figure 38 and the pressure distribution plots of the experimentally measured pressures opposed to the CFD results in the plots 7 – 9.

Figure 38: Pressure strips on the FS.14 rear wing

According to the plots below, second and third elements of the wing might undergo flow separation. Another probability is that the elements are

underperforming due to lower air energy than predicted by the CFD simulations. As for the first element, it shows curious suction peaks at several spots. We assume that the peaks could be caused by the wing skin deformation around the inner supporting ribs. That is why we decided to develop a full core for all elements for the next season. Another reason of the deviations could be the influence of the sensors, wires, connectors and tape on the airflow.

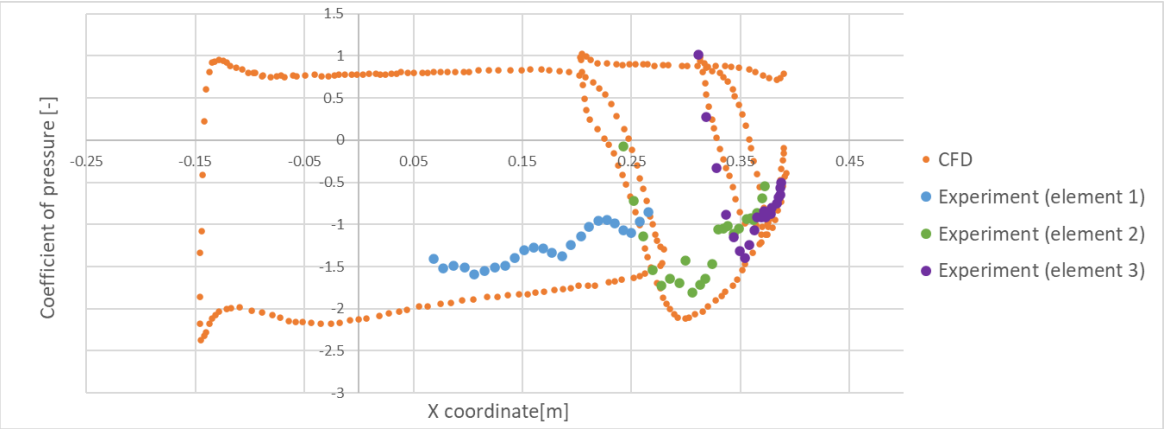

Plot 7: Pressure distribution in the left section of the wing as measured and predicted by CFD

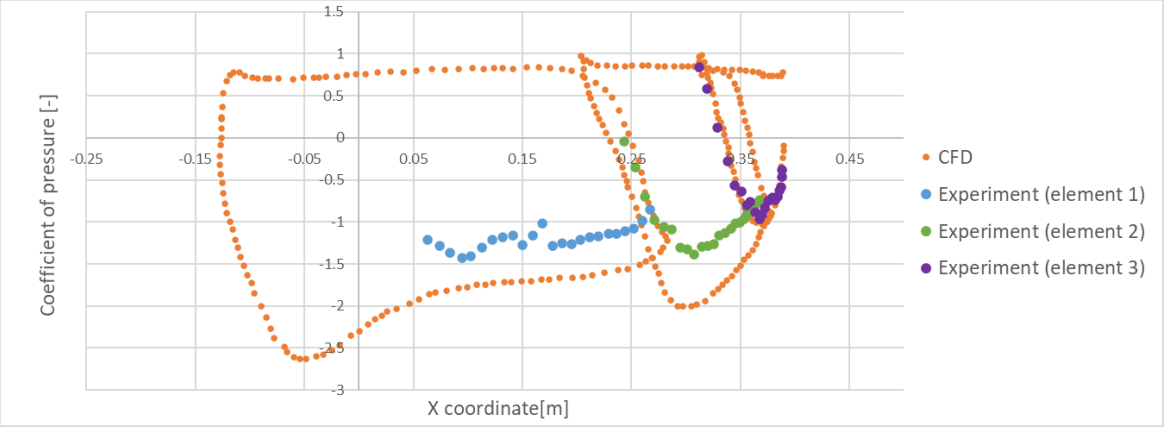

Plot 8: Pressure distribution in the middle section of the wing as measured and predicted by CFD

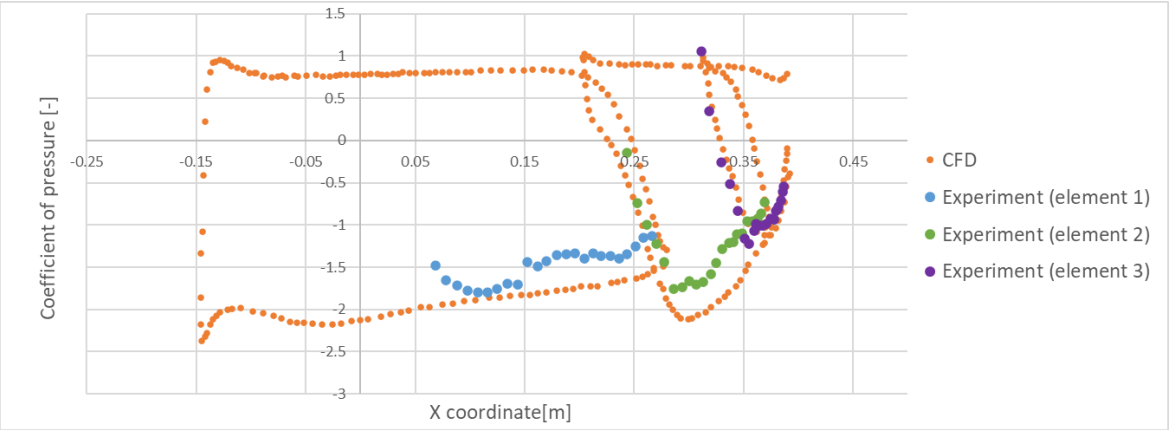

Plot 9: Pressure distribution in the right section of the wing as measured and predicted by CFD

7.2 Cotton thread test

Another test aimed to study the wing behaviour was the cotton thread test. Multiple pieces of cotton thread were attached to the lower side of the wing with thin tape. The wing was then filmed during a track drive using a camera attached to the end plate. The threads stayed close to the wing surface during the whole drive, indicating attached flow.

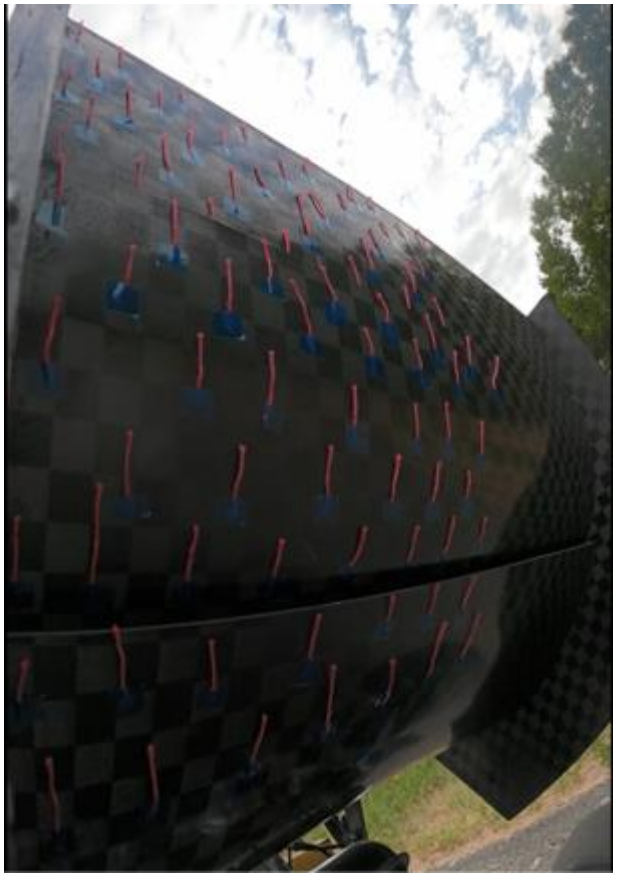

Figure 39: Cotton strings on the suction side of the FS.14 rear wing

8 Conclusion

The development and manufacturing of the rear wing for the FS.14 can be considered successful. The goals set for the overall vehicle performance were met, and we managed to manufacture a reliable assembly within a short time period. Considering drastic changes to the concept and a strong focus on the aerodynamic performance, the goals set for the next rear wing were mainly set on the manufacturing: the choice of lighter carbon fibre layups, cores and adhesives, more affordable, precise and time-efficient manufacturing technologies.

List of used literature

[1] CTU CarTech [online]. CTU CarTech, quote [10.12.2023]. Available at https://ctucartech.cz/en/

[2] Formula SAE. FSAE History [online]. FSAE, quote [10.12.2023]. Available at https://www.fsaeonline.com/page.aspx?pageid=c4c5195a-60c0-46aa-acbf-2958ef545b72

[3] Formula Student Germany. FSG Rules & Important Documents [online]. FSG, quote [10.12.2023]. Available at https://www.formulastudent.de/fsg/rules/

[4] Rennstall Esslingen. Stallardo'21 [online]. Rennstall Esslingen, quote [10.12.2023]. Available at https://rennstall-esslingen.de/fuhrpark-2/stallardo21-2/

[5] KATZ, Joseph. Race car aerodynamics: designing for speed. Cambridge, MA, USA: R. Bentley, c1995. ISBN 0837601428.

[6] ŠEVČÍK, Martin. Aerodynamics design methodology of Formula Student car. Czech Technical University in Prague, Prague, Czech Republic, 2021 https://dspace.cvut.cz/handle/10467/97330

[7] Airfoil tools. S1223 [online]. Airfoil tools, quote [10.12.2023]. Available at http://airfoiltools.com/airfoil/details?airfoil=s1223-il

[8] KLIER, Filip. Aeropackage design and manufacturing optimization. Czech Technical University in Prague, Prague, Czech Republic, 2022 https://dspace.cvut.cz/handle/10467/107147

List of figures

List of tables

List of plots